Nuclear Data for Science and Technology (1988 MITO), 963- 966, Copyright © 1988 JAERI.

STUDY OF $^{249}Cf(n_{th},f)$ WITH LOHENGRIN MASS SEPARATOR

M. Djebara[1], M. Asghar[1], J.P. Bocquet[2], R. Brissot[3], J. Crançon[3], Ch. Ristori[3], E. Aker[3], D. Engelhardt[4], B.D. Wilkins[5] and U. Quade[6]

1) I. Ph. USTHB, B.P. 32, El Alia, Alger, Algérie
2) ILL, 156X, 38042 Grenoble, France
3) CEN-DRF/SPH/PhAN, 85X, 38041 Grenoble, France
4) T.U.K., 7500 Karlsruhe, West Germany
5) A.N.L., Argonne, Illinois 60439, USA
6) University of Munich, West Germany

Abstract: The ILL-Grenoble mass separator Lohengrin was used to measure the yields of light fission products from $^{249}Cf(n_{th},f)$ as a function of A, Z, the kinetic energy and the ionic charge states. The mass range covered, for E_{Loh}=87 to 112 MeV, was A_L = 89 to 120. The charge polarisation $\Delta Z(A_L) = Z - Z_{UCD}$ was deduced. The proton and neutron odd-even effects were found to be δ_p = (4.6 + 0.7)% and δ_n = (9.5 + 0.7)%. The odd-even effects on mean proton and neutron total kinetic energy are $\delta E_k^{o-e}(p)$ = (0.20 + 0.07) MeV and $\delta E_k^{o-e}(n)$ = (0.48 + 0.16) MeV. The mean value of isobaric variance $\langle\sigma_Z^2\rangle$ = (0.43 + 0.03). These results and the different distributions are compared with the existing data on the other fissioning nuclei.

Introduction

Over the past 15 years, the recoil mass spectrometer Lohengrin /1/ has been extensively used to measure the mass, nuclear charge and kinetic energy distributions for different fissioning nuclei /2-5/ produced through thermal neutron absorption. In this paper, we present the results on these distributions for $^{249}Cf(n_{th},f)$ obtained with this instrument. This is the heaviest fissioning system studied so far with this spectrometer.

Experimental Set-up and Measurements

A mass resolution of $\frac{A}{\Delta A} \approx 400$ (FWHM) was chosen for Lohengrin. The mass yields were measured by setting the spectrometer condensor at fixed high voltages and then scanning the A/q with the magnetic field. The different masses contributing to a A/q line and the masses of different, but not resolved A/q lines could be separated because of their different kinetic energies with the high resolution ionisation chamber installed at the exit slit /6/. The nuclear charge distribution for a given A/q was determined by measuring the residual energy behind a 70 mm x 3 mm parylene C absorber with the ionisation chamber. The mass yields for mass numbers 88 < A < 120 were measured for 7 fission product kinetic energies: E_{Loh} = 87, 91, 95, 99, 103, 107 and 112 MeV. For 91, 99 and 107 MeV these mass yields were measured for 4 to 6 ionic charge states for each of the fission product mass. For the other energies, the yield for each mass was measured for only one ionic charge state. A linear interpolation and extrapolation was used to construct the yield matrix $Y(A,E_{Loh},q)$. The isobaric charge distributions were measured for 6 kinetic energies E_{Loh} = 91, 95, 99, 103, 107 and 112 MeV, and for 1 to 4 ionic charge states for each mass.

Data Analysis

The "burn up" data, Fig. 1, were used to correct the counting rates at different energies as a function of time and to get the absolute mass yields.

The residual kinetic energy data from the ionisation chamber were analysed into relative yields of Z components with a sum of gaussians. This analysis led to the yield surface $Y_{rel}(A, Z, E_{Loh}, q)$, which was transformed into the absolute yield matrix $Y(A, Z, E_{Loh}, q)$ with the help of the yield matrix $Y(A, E_{Loh}, q)$. Then, the E_{Loh} were corrected for the energy loss in the target and the Ni-foil covering the target, as a function of A and Z using the semi-empirical relations of Ziegler /7/. This procedure helped us to get the surface Y(A, Z, E, q), where E is the corrected kinetic energy.

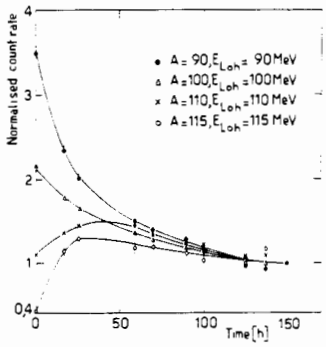

Fig. 1: The "burn up" for different E_{Loh}. The counting rates are normalised to one at t = 150 h after the introduction of the target.

Results and Discussion

Energy-integrated Mass Distribution

The energy-integrated mass distribution Y(A) from this work is shown in Fig. 2. The Lohengrin mass yields on the lower side of the yield peak are, on the average, ∿5% higher than the corresponding Cosi fan tutte spectrometer values /8/, which are consistent with the radiochemical data /9/.

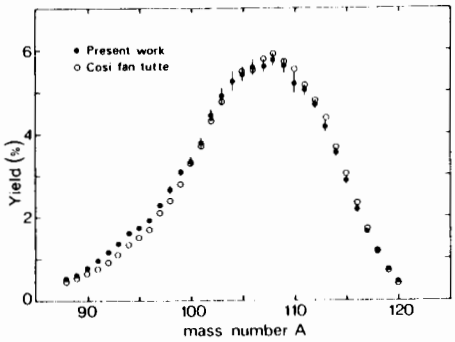

Fig. 2: Mass distribution integrated over the kinetic energy distributions of fragments

Kinetic Energy Distributions of Fragments $Y(E)|_A$

The average kinetic energies of fragments and their dispersions are determined through the first and the second moments of the energy distributions $Y(E)|_A$. They are shown in Figs. 3 and 4 along with the corresponding values from Cosi.

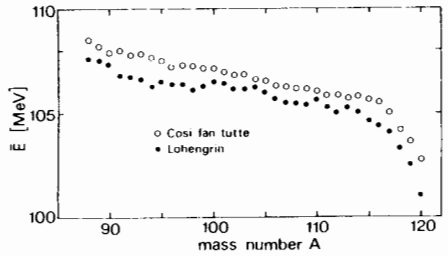

Fig. 3: The fragment mean kinetic energy $\bar{E}$ as a function of fragment mass

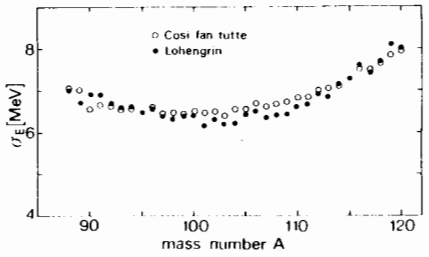

Fig. 4: The rms of fragment kinetic energy σ_E as a function of fragment mass

The Lohengrin $\bar{E}(A)$ are $\approx$ 0.5 - 1 MeV lower than the Cosi results. Moreover, although the $\bar{E}(A)$ distribution from Cosi is quite smooth, the $\bar{E}(A)$ distribution from Lohengrin shows weak oscillations around masses 100, 104 and 110.

The Mean Nuclear Charge

Fig. 5 gives $\Delta Z = Z_{UCD} - \bar{Z}$, integrated over the kinetic energy distribution, as a function of the primary fragment masses A'. One observes that $\Delta Z(A')$ reaches the mass symmetry within $\approx$ 2 mass units. Apart from this result on ^{250}Cf, only in

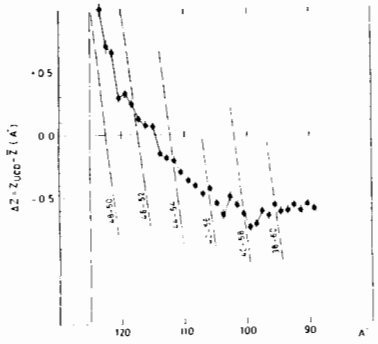

Fig. 5: The variation of $\Delta Z = Z_{UCD} - \bar{Z}$, integrated over the kinetic energy distribution as a function of the primary fragment mass A'

the case of $^{235}U(n_{th},f)$, the $\Delta Z(A')$ values reach the mass symmetry /10/. The behaviour of $\Delta Z(A')$ is quite different for the two fissioning nuclei. In the case of ^{236}U, there is an indication of a stabilizing effect of the Z=50 spherical shell in the heavy fragment. Here the value of $\Delta Z(A')$ passes the $\Delta Z(A')=0$ line right in the middle of the Z=50 shell at $A'_H \approx 128$; it continues to increase linearly as A' increases and reaches a maximum value of $\Delta Z \approx 0.6$ at $A'_H \approx 126$ and, thereafter, it decreases linearly over $\approx$ 8 mass units to become zero at symmetry. In the case of ^{250}Cf $\Delta Z(A')$ remains practically constant ≈ -0.6 for $A'_L < 105$. It starts to increase for $A' > 105$ and passes the $\Delta Z(A') = 0$ line at $A'_L \approx 115$, which is $\approx$ 7.5 mass units away from the center of the Z=50 shell. It continues to increase up to $A'_L \approx 123$, where $\Delta Z \approx 1$, but without ever crossing the Z=50 shell.

In the case of ^{250}Cf, when the heavy fragment contains 50 protons, the complementary light fragment with Z=48 has also entered the Z=50 spherical shell region. Therfore, there may not be any stabilization due to this shell for ^{250}Cf as in the case of ^{236}U.

Variance of Nuclear Charge Distribution $\langle\sigma_Z^2\rangle$

Fig. 6 shows $\langle\sigma_Z^2\rangle$ averaged over all the masses, as a function of the kinetic energy along with the results for ^{236}U, ^{239}Np and ^{240}Pu. One observes that although $\langle\sigma_Z^2\rangle$ for ^{236}U and ^{240}Pu decreases as the kinetic energy increases, they are practically constant for ^{239}Np and ^{250}Cf. It was

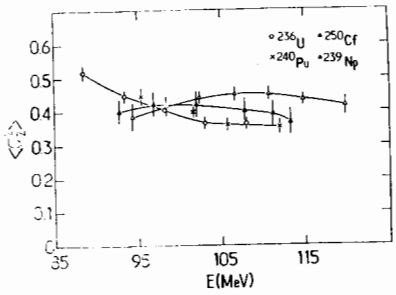

Fig. 6: The variation of $\langle\sigma_Z^2\rangle$, integrated over the measured mass range, as a function of kinetic energy of fragments

shown /3/ that the behaviour of $\langle\sigma_Z^2\rangle$ as a function of kinetic energy, for ^{236}U and ^{240}Pu could be accounted for by neutron emission from the fragments that decreases as their kinetic energy goes up. However, the results for ^{239}Np and ^{250}Cf do not support this idea. We feel that the behaviour of $\langle\sigma_Z^2\rangle$ as a function of kinetic energy for ^{236}U and ^{240}Pu comes about prinicpally from the proton odd-even effect. The nearly constant values of $\langle\sigma_Z^2\rangle$ for ^{239}Np and ^{250}Cf result from the fact that there is no proton odd-even effect in the case of the odd-Z fissioning ^{239}Np nucleus and it is quite small in the case of ^{250}Cf.

A constant value of $\langle\sigma_Z^2\rangle = 0.40 \pm 0.05$ covers all the $\langle\sigma_Z^2\rangle$ values for the four fissioning nuclei of Fig. 6. This is a significant result. It has been shown /11/ that $\langle\sigma_Z^2\rangle$ results from zero-point oscillation of a collective isovector giant dipole resonance of the composite system at the exit point which represents the physical scission point. Since the scission configurations of different nuclei from Th to Cf are practically identical, the $\langle\sigma_Z^2\rangle$ should be similar for all the fissioning systems as is the case. These results show in an almost direct way that the scission configuration is a compact entity.

Proton Odd-even Effect in Yields δp and in Kinetic Energies δE_K^{o-e}

The mean proton odd-even effect from the elemental yields integrated over the kinetic energy is

$$\delta p = \sum_{35<Z<48} (Y_{eZ} - Y_{oZ}) = (4.6 \pm 0.7)\%.$$

This is the first time that δp has been determined for $^{249}Cf(n_{th},f)$. Table 1 gives the δp values along with some other data for all the fissioning nuclei, produced through thermal neutron absorption, studied so far. One notices that δp decreases from ≈ 40% for ^{230}Th to 4.6% for ^{250}Cf. The relation (Fig. 7):

$$\delta p|\%| = a\, e^{-bz}$$

represents very well the δp data for different nuclei. Here $z = Z_F^2/A^{1/3}$, is the Coulomb parameter and the constants $a = e^{17.496}$ and $b = 0.0105$. We have also tried to correlate the δp data with the fissibility parameter $x = Z_F^2/A_F$, but this representation is proorer than that with z. Furthermore,

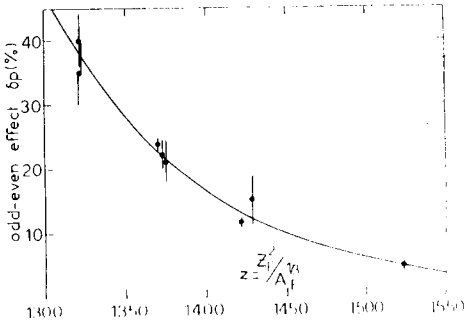

Fig. 7: The fit of $\delta p|\%|$ data to the Coulomb parameter $z = Z_F^2/A_F^{1/3}$, through the relation $\delta p|\%| = a\, e^{bz}$.

we have found that $Q_F(A_F)$, $E_K(A_F)$, already known, and the saddle-to-scission energies $E_{SS}(A_F)$ /11/ vary linearly with z, but this is not the case with the fissibility parameter x. It is reasonable to think that, in the saddle-to-scission region, the intrinsic excitation increases with z leading to an exponential lowering of δp with this parameter.

Fig. 8 shows the variation of proton odd-even effect in yield with kinetic energy for ^{236}U, ^{240}Pu and ^{250}Cf. One observes a decrease in the slopes of the curves as one moves from ^{236}U to ^{250}Cf; this may be linked to the excitation energy

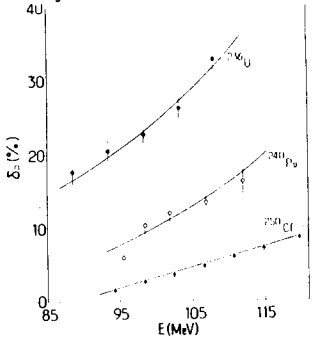

Fig. 8: The variation of δn as a function of fragment kinetic energy

available, at the last saddle, to the fissioning nucleus, and this energy increases from ^{236}U to ^{250}Cf.

We deduced the mean odd-even effect on kinetic energy in the charge range 36 < Z < 44, which is not effected by shell effects as

$$\delta E_K^{o-e} = (0.20 \pm 0.07)\ \text{MeV}.$$

Neutron Odd-even Effect δn in Yields

The mean neutron odd-even effect in the yields integrated over kinetic energy is

$$\delta n = \sum_{52 \le N \le 73} \frac{(Yen - Yon)}{(Yen + Yon)} = (9.5 \pm 0.7)\%$$

As table 1 shows δn increases from 5.4% for ^{236}U to 9.5% for ^{250}Cf; most of it ought to be linked to the evaporation of prompt neutrons from the fragments since $\bar{\nu}_T$ increases from 2.4 for ^{236}U to 4.4 for ^{250}Cf.

Fig. 9 gives the dependence of δn on fragment kinetic energy along with the ^{236}U and ^{240}Pu results. In the case of ^{250}Cf, the δn increases by about a factor of 2 over the kinetic energy range covered.

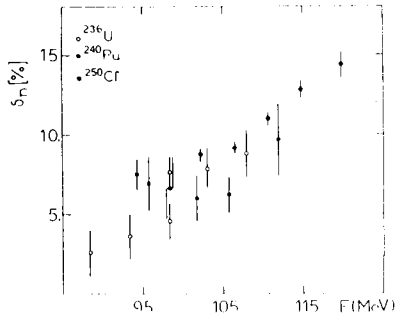

Fig. 9: The variation of δn as a function of fragment kinetic energy

In Fig. 10 we present the local δn as a function of N for energy-integrated isotonic yields. The δn curves show strong peaks centred at N ≈ 59.5 and ∿ 66.5, and δn increases sharply beyond N ≳ 69.5. We have simulated the evaporation of neutrons with a Monte Carlo programme. The calculated curve (preliminary) also presented in Fig. 10, reproduces just about the experimental data, though the calculated peak positions are shifted down relative to the experimental peaks by ≈ 3 neutrons.

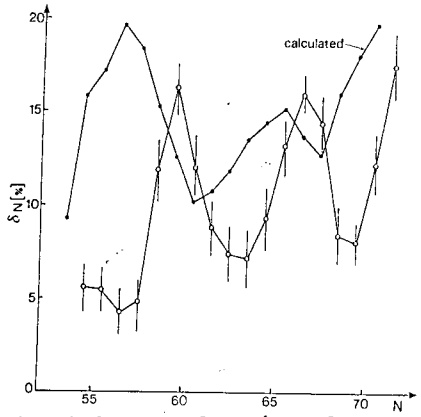

Fig. 10: The mean local δ_n as a function of N. The calculated curve is from a Monte Carlo simulation of neutron evaporation

TABLE 1

Some pertinent data for ^{230}Th, ^{233}U, ^{235}U, ^{236}U, ^{239}Pu, ^{240}Pu and ^{250}Cf Fissioning nuclei

	^{230}Th	^{233}U	^{235}U	^{236}U	^{239}Pu	^{240}Pu	^{250}Cf
$\sigma_{n,f}$[b]	30.5 ± 3	75.2 ± 4.7	531.1 ± 1.2	582.2 ± 1.2	16.5 ± 0.5	742.5 ± 3	1060 ± 50
B_n[MeV]	6.78	6.79	6.84	6.54	6.06	6.52	6.62[a]
inner barrier V_a[MeV]	6.1	5.8	5.6	5.62	6.3	5.57	5.6
outer barrier V_b[MeV]	6.5	5.8	5.5	5.53	5.7	5.07	5.6
excitation energy above $V_b = (B_n - V_b)$ [MeV]	0.28	≈ 0.0	1.34	1.01	≈0.0	1.45	1.02
charge odd-even effect δ_p[%]	40 ± 4[b]	21 ± 2[b]	22.1 ± 2.1[c]	23.2 ± 0.7[c]	14 ± 3[d]	11.6 ± 0.6[c]	4.6 ± 0.7
neutron odd-even effect δ_n[%]	35 ± 5[b]		5.4 ± 1.7[d]	5.4 ± 0.7[d]		6.46 ± 0.7[f]	9.5 ± 0.7

a) Ref. 12) b) Ref. 13) c) Ref. 14) d) Ref. 2) e) Ref. 3) f) Ref. 5) g) Ref. 15).

Conclusion

The recoil mass spectrometer Lohengrin has been used to study $^{249}Cf(n_{th},f)$. The principal results are:

a) The mean mass distribution is rather smooth and structureless.
b) The behaviour of $\Delta Z(A') = Z_{UCD}(A') - \bar{Z}(A')$, differs strongly from that for $^{235}U(n_{th},f)$.
c) The isobaric variance $\langle\sigma_Z^2\rangle$ shows little dependence on kinetic energy. Its mean value is (0.43±0.03).
d) The mean $\delta p = (4.6 \pm 0.7)\%$, and it increases with fragment kinetic energy.
e) The mean $\delta n = (9.5 \pm 0.7)\%$, and it increases strongly with fragment kinetic energy. It seems that most of δn results from prompt neutron evaporation from the fragments.

REFERENCES

1. E. Moll, H. Schrader, G. Siegert, M. Asghar, J.B. Bocquet, G. Bailleul, J.P. Gautheron, J. Greif, G.I. Crawford, C. Chauvin, H. Ewald, H. Wollnik, P. Armbruster, G. Fiebig, H. Lawin and K. Sistemich, Nucl. Instr. et Meth., 123, 615 (1975)
2. U. Quade, Ph.D. Thesis, University of Munich (1983)
3. W. Lang, H.G. Clerc, H. Wohlfarth, H. Schrader and K.H. Schmidt, Nucl. Phys. A345, 34 (1980)
4. Lohengrin Collaboration: G. Martinez, Ph.D. Thesis, University of Bordeaux; W. Arafa, Ph.D. Thesis, University of Grenoble (1986)
5. C. Schmitt, A. Guessons, J.P. Bocquet, H.G. Clerc, R. Brissot, D. Engelhardt, H.R. Faust, F. Gönnenwein, M. Mutterer, H. Nifenecker, J. Pannicke, Ch. Ristori and J.P. Theobald, Nucl. Phys. A430, 21 (1984)
6. J.P. Bocquet, R. Brissot and H. Faust (to be published)
7. J.F. Ziegler, "Handbook of stopping cross sections for energetic ions in all elements", Pergamon Press, 1980
8. Cosi fan tutte collaboration: E. Aker, Ph.D. Thesis, University of Karlsruhe (1987)
9. J.K. Dickens and J.W. McConnell, Phys. Rev. (24, 192 (1981))
10. A.C. Wahl, Phys. Rev. C32, 184 (1985)
11. M. Asghar, Z. Phys. A 296, 79 (1980); M. Asghar and R.W. Hasse, J. Phys. C6, 455 (1984)
12. S. Bjornholm and J.E. Lynn, Rev. Mod. Phys. 52, 725 (1980)
13. M. Djebara, M. Asghar, J.P. Bocquet, R. Brissot, M. Maurel, H. Nifenecker and Ch. Ristori, Nucl. Phys. A425, 120 (1984)
14. G. Mariolopoulos, Ch. Hamelin, J. Blachot, J.P. Bocquet, R. Brissot, J. Crançon, H. Nifenecker and Ch. Ristori, Nucl. Phys. A361, 213 (1981)
15. M. Haddad, J. Crançon, G. Lhospice and M. Asghar, Nucl. Phys. (in press)